Acta Mech
https://doi.org/10.1007/s00707-022-03159-w

ORIGINAL PAPER

Jian En Chen · Timo Theurich · Malte Krack · Themistoklis Sapsis · Lawrence A. Bergman · Alexander F. Vakakis

Intense cross-scale energy cascades resembling "mechanical turbulence" in harmonically driven strongly nonlinear hierarchical chains of oscillators

Received: 2 September 2021 / Revised: 10 December 2021 / Accepted: 23 January 2022

Abstract In the present study, the dynamics of one- and two-degree-of-freedom linear oscillators attached to hierarchical chains of oscillators coupled by strongly nonlinear cubic springs in parallel with viscous dampers are investigated. The mass, stiffness, and damping properties of the nonlinear oscillators are specified to follow a certain scaling rule, in such a way that their mass, stiffness, and damping properties decrease along the chain. The linear oscillators are driven harmonically near to their primary resonances. For sufficiently low excitation levels, linear behavior prevails leading to nearly harmonic responses, where the mechanical energy remains localized in the directly forced linear oscillator. For sufficiently high excitation level (that is, above a critical level of the forcing amplitude), however, the system responds in a chaotic way, where a substantial part of the energy is transferred across the hierarchical nonlinear chain in an energy cascade. Interestingly, there exist "chaotic bands" where all cubic oscillators are simultaneously activated or deactivated depending on the frequency; hence, a chaotic synchronization occurs in the system. When energy cascading is initiated the smaller-scale cubic oscillators become driven by the chaotic dynamics of the larger-scale cubic oscillators. Once the oscillator chain enters the chaotic response regime, the pattern of nonlinear energy cascading resembles (but is not identical to) the –5/3 Kolmogorov energy cascading power law observed in fully developed turbulence. Similarities and differences in the observed mechanical energy cascades and those realized in turbulent flows are discussed.

1 Introduction

Turbulent flow is a prime example of cross-scale energy transfer in nature, where large unstable vortices break up into few smaller vortices, thereby transferring the kinetic energy from larger scales to smaller ones in a well-known energy cascade corresponding to irreversible energy transfers from large to small scales. Studies of mathematical models of such energy cascades indicated that they are generated by the combined effects of instabilities of the large-scale vortices and the quadratic nonlinearity of the governing Navier–Stokes

J. E. Chen (✉)
Tianjin Key Laboratory for Advanced Mechatronic System Design and Intelligent Control, Tianjin University of Technology, Tianjin, People's Republic of China
e-mail: vchenje@163.com

T. Theurich · M. Krack
Institute for Aircraft Propulsion Systems, University of Stuttgart, Stuttgart, Germany

T. Sapsis
Mechanical Engineering, Massachusetts Institute of Technology, Cambridge , USA

L. A. Bergman
Aerospace Engineering, University of Illinois, Urbana, USA

A. F. Vakakis
Mechanical Science and Engineering, University of Illinois, Urbana, USA

Published online: 13 March 2022

equations [1, 2]. Studies show that simultaneous energy dissipation occurs over many scales, leading to the so-called super dissipation efficiency of turbulence. Motivated by the cross-scale nonlinear energy transfers in turbulent flows, the problem of inducing similar predictable designs of passive nonlinear targeted energy transfers in mechanical and structural systems has been the topic of current works, e.g., [3]. A review of the literature reveals that the nonlinear energy transfer principle has been applied in numerous applications, including vibration isolation and absorption [4–6], energy harvesting [7, 8], and passive guidance of the energy flow [9, 10].

Considering the complexity of turbulent flows, several phenomenological models such as the shell model [11] and its modified versions [12] have been proposed to simulate the features of energy cascades and chaotic dynamics in turbulence. With the continuous upgrading of the aforementioned models, the construction of phenomenological models of turbulent flows has become an important study direction. Recently, a linear oscillator chain was used to reproduce the energy spectrum with the well-known Kolmogorov power law [13, 14], and an analogous study was performed between a weakly nonlinear chain and turbulence [15].

Additional works studied wave turbulence in the acoustics of elastic plates [16–18]. In [16] the nonlinear energy transfers between propagating waves in a thin elastic plate were studied employing the Föppl–von Kármán theory for thin plates; an energy scaling law for the resulting energy cascades was then derived which was analogous to Kolmogorov's scaling law for fully developed turbulent flows. This study was extended in [17] where the same thin-plate model was used to develop a theoretical phenomenological model for the time–frequency dependence of the power spectrum of thin vibrating plates in the wave turbulence regime. Interestingly, the analysis provided self-similar universal solutions relating the power spectrum to both the input power and the dissipative capacity of the plates. Additional works provided experimental investigations of wave turbulence in plates, e.g., [19] and [20].

An additional aspect studied in this work is the issue of chaotic synchronization of a chain of nonlinear oscillators as system parameters (e.g., excitation amplitude or frequency) change. Synchronization is a universal feature of nonlinear dynamical systems [21], e.g., ranging from synchronous variations of cell nuclei and firing of neurons, to normal or abnormal synchronization of heart rates with respiration rhythms, and cooperative social behaviors of humans [21]. Whereas synchronization is typically related to coupled dynamical systems undergoing some sort of resonance, chaotic systems can synchronize as well [22], in which case a clear criterion for assessing such chaotic synchronization can be formulated by Lyapunov exponents. In this work, an interesting chaotic synchronization phenomenon is presented, whereby, as the frequency of an applied excitation increases, an entire chain of strongly nonlinear oscillators initially in a low-amplitude linearized dynamical state, suddenly "bursts" into finite-amplitude synchronized chaotic response. Further increase of the frequency beyond a certain critical threshold leads to sudden de-synchronization of the chaotic response, with all oscillators simultaneously returning to a low-amplitude linearized response regime. It is precisely this chaotic synchronization that gives rise to sustained nonlinear energy cascades in the nonlinear chain, resembling "mechanical turbulence."

Specifically, in the present study, nonlinear oscillator chains composed of at least one linear oscillator attached to a hierarchical chain of purely cubic oscillators are considered. In comparison with constructing phenomenological models of turbulent flows, it was intended to establish the governing law of the resulting nonlinear energy cascades and energy transfers in the oscillator chains analogous to those occurring in turbulent flows, and then guiding the design for such "mechanical turbulence" features in practical engineering applications. To this end, nonlinear energy cascades and energy transfers in the studied oscillator systems in the regime of chaotic responses are investigated. The main aim is to show that robust energy cascades can be predictably induced in hierarchical nonlinear oscillator chains and provide methods to quantify and study these uni-directional (irreversible) energy transfers.

2 Problem formulation and analysis method: Case of single linear oscillator

The first system considered is depicted in Fig. 1, composed of a grounded linear oscillator with mass M, stiffness K, viscous damping coefficient μ, and an attached hierarchical chain of N strongly nonlinear oscillators; each oscillator in the chain is coupled to its neighbors by a purely cubic stiffness in parallel to a viscous damper, with m_n, k_n, and λ_n ($n = 1, \ldots, N$) denoting the mass, stiffness, and damping coefficients, respectively. An important feature of the attached chain of nonlinear oscillators is that it is hierarchical, i.e., the mass, stiffness, and damping of each oscillator decrease according to a specified scaling law from left to right. Moreover, the displacements of the $N + 1$ oscillators of the system are denoted by x_{n+1}, $n = 0, 1, \ldots, N$. Lastly,

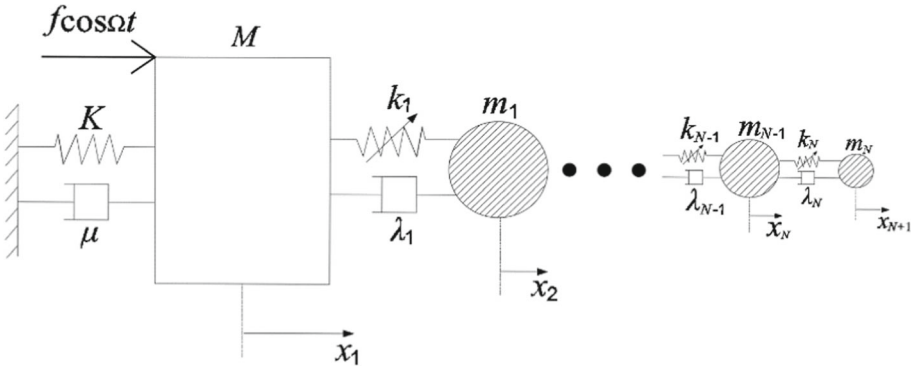

Fig. 1 A grounded linear oscillator attached to a hierarchical chain of N ungrounded strongly nonlinear oscillators with purely cubic stiffness characteristics

a harmonic excitation represented by $f\cos(\Omega t)$ is applied to the linear oscillator, where f and Ω are the excitation amplitude and frequency, respectively.

The governing equations of motion for the system of Fig. 1 can be expressed in dimensional form as

$$M\ddot{x}_1 + \mu\dot{x}_1 + Kx_1 + \lambda_1(\dot{x}_1 - \dot{x}_2) + k_1(x_1 - x_2)^3 = f\cos(\Omega t), \tag{1.1}$$

$$\begin{aligned} m_n\ddot{x}_{n+1} &+ \lambda_n(\dot{x}_{n+1} - \dot{x}_n) + k_n(x_{n+1} - x_n)^3 \\ &+ \lambda_{n+1}(\dot{x}_{n+1} - \dot{x}_{n+2}) + k_{n+1}(x_{n+1} - x_{n+2})^3 = 0, n = 1,\ 2\ \cdots\ N-1, \end{aligned} \tag{1.2}$$

$$m_N\ddot{x}_{N+1} + \lambda_N(\dot{x}_{N+1} - \dot{x}_N) + k_N(x_{N+1} - x_N)^3 = 0. \tag{1.3}$$

Introducing the normalized variables and parameters,

$$\varepsilon_n = \frac{m_n}{M}, \tilde{t} = \sqrt{\frac{K}{M}}t, \tilde{\mu} = \frac{\mu}{\sqrt{KM}}, \tilde{\lambda} = \frac{\lambda}{\sqrt{KM}}, \tilde{k}_n = \frac{k_n}{K}, \tilde{f} = \frac{f}{K}, \tilde{\Omega} = \sqrt{\frac{M}{K}}\Omega,$$

the equations of motion are expressed in the following non-dimensional form:

$$\ddot{x}_1 + \tilde{\mu}\dot{x}_1 + x_1 + \tilde{\lambda}_1(\dot{x}_1 - \dot{x}_2) + \tilde{k}_1(x_1 - x_2)^3 = \tilde{f}\cos(\tilde{\Omega}\tilde{t}), \tag{2.1}$$

$$\begin{aligned} \varepsilon_n\ddot{x}_{n+1} &+ \tilde{\lambda}_n(\dot{x}_{n+1} - \dot{x}_n) + \tilde{k}_n(x_{n+1} - x_n)^3 \\ &+ \tilde{\lambda}_{n+1}(\dot{x}_{n+1} - \dot{x}_{n+2}) + \tilde{k}_{n+1}(x_{n+1} - x_{n+2})^3 = 0,\ n = 1,\ 2\ \cdots\ N-1, \end{aligned} \tag{2.2}$$

$$\varepsilon_N\ddot{x}_{N+1} + \tilde{\lambda}_N(\dot{x}_{N+1} - \dot{x}_N) + \tilde{k}_N(x_{N+1} - x_N)^3 = 0, \tag{2.3}$$

where, for convenience, the tildes will be dropped in the subsequent analysis. The dynamics of system (2) is computed by explicit time step integration using the Runge–Kutta method in Matlab® subject to zero initial conditions. Subsequently, the steady-state dynamical response is analyzed with particular focus on the partition of energy along the system from which energy transfer phenomena can be inferred. Indeed, when the system is excited at steady state (i.e., after the initial transients have dissipated), a portion of the energy is expected to be dissipated by viscous damping, while the rest of the energy should be transferred throughout the oscillator chain as it reaches dynamical equilibrium. Clearly, the transferred energy should appear as kinetic and potential energies of the constituent oscillators of the system, and one of the main objectives of the study is to investigate the irreversible nonlinear energy transfer from the large-scale linear oscillator to the smaller scale hierarchical strongly nonlinear oscillators. Accordingly, certain energy measures are defined.

First, the average energy in the linear (E_{LO}) and nonlinear oscillators (E_n) at steady state are expressed as

$$E_{LO} = \frac{1}{T}\int_{t_0}^{t_0+T}\left(\frac{1}{2}(\dot{x}_1^2 + x_1^2) + \frac{1}{8}k_1(x_1 - x_2)^4\right)dt, \tag{3.1}$$

$$E_n = \frac{1}{T}\int_{t_0}^{t_0+T}\left(\frac{1}{2}\varepsilon_n\dot{x}_{n+1}^2 + \frac{1}{8}k_n(x_n - x_{n+1})^4 + \frac{1}{8}k_{n+1}(x_{n+1} - x_{n+2})^4\right)dt,$$

$$n = 1,\ 2, \ldots,\ N, \tag{3.2}$$

where T is a specified time interval after the system reaches steady state, and t_0 signifies the initial time instant of the computation. Note that the portion of the potential energy stored in the cubic springs of the hierarchical nonlinear oscillators is associated with both connecting stiffnesses with its neighboring oscillators.

In addition, the input energy flux (E_{in}) and normalized energy flux ($\hat{E}_n$) between neighboring nonlinear oscillators at steady state are defined as follows:

$$E_{in} = \int_{t_0}^{t_0+T} f\cos(\Omega t)\,\dot{x}_1\,dt, \tag{4.1}$$

$$\hat{E}_n = \frac{1}{E_{in}\varepsilon_n}\int_{t_0}^{t_0+T} k_n(x_n - x_{n+1})^3\dot{x}_{n+1}\,dt,\ n = 1,\ 2, ..., N. \tag{4.2}$$

Specifically, the input energy flux (4.1) is computed as the integral over a period of the excitation of the power input provided by the force to the primary oscillator, $f\cos(\Omega t)\,\dot{x}_1$. Similarly, the normalized energy flux (4.2) quantifies the energy that the $(n+1)-th$ oscillator receives from its neighboring $n-th$ oscillator, and is computed as the integral over a period of the excitation of the power provided by the nonlinear coupling stiffness force to the $(n+1)-th$ oscillator, $k_n(x_n - x_{n+1})^3\dot{x}_{n+1}$. Here, only the non-dissipative nonlinear coupling forces (exerted by the cubic stiffnesses) are considered, but not the linear viscous dissipative coupling force since this is a dissipator (instead of a propagator) of power through the chain.

It turns out that provided the forcing amplitude is above a critical threshold the strong (in fact non-linearizable) stiffness nonlinearities in the hierarchical oscillator chain play a role, and chaotic steady-state dynamics occur; on the contrary, for sufficiently small forcing amplitudes regular (periodic) steady-state responses are realized. To distinguish regular from chaotic responses and further characterize the chaotic dynamics, Lyapunov exponents are computed and analyzed as detailed later. In the following numerical simulations, a nonlinear hierarchical chain composed of $N = 8$ coupled cubic oscillators is studied. The hierarchy of scales (i.e., from large-scale to small scale nonlinear oscillators) is achieved by decreasing the system parameters from the first ($n = 1$) to the last ($n = N$) oscillator according to the scaling laws,

$$\frac{\varepsilon_{n-1}}{\varepsilon_n} = 5,\ \frac{k_{n-1}}{k_n} = 50,\ \frac{\lambda_{n-1}}{\lambda_n} = 2,\ n = 2,\ 3, \ldots, N,$$

with the system parameters of the linear oscillator and the first cubic oscillator given by μ=0.01, ε_1=0.04, $k_1 = 0.3$, and λ_1=0.000128. Hence, a transition from the larger scale directly excited linear oscillator to smaller scale attached strongly nonlinear oscillators is introduced.

3 Results: case of a single linear oscillator

In Fig. 2 the frequency response plots of the nine oscillators of the system are presented for weak (Fig. 2a) and strong (Fig. 2b) excitation levels. In these plots the average energies of the oscillators at steady state are depicted as functions of the excitation frequency Ω for constant excitation amplitude f. Considering first the case of weak harmonic excitation corresponding to $f = 0.001$ in Fig. 2a, the response of the linear oscillator is periodic with frequency identical to the frequency of the excitation; accordingly the frequency response plot is similar to the damped resonance plot that is encountered when a single linear oscillator is forced by a harmonic excitation. At the same time the energy levels of the cubic oscillators are negligible so at steady state the energy is almost entirely localized to the directly excited linear oscillator. Hence, for sufficiently low excitation levels, linear behavior prevails, leading to a nearly harmonic dynamical response of the linear oscillator.

A radically different picture, however, is noted when the force excitation level is increased. Figure 2b depicts four frequency response curves corresponding to the linear and the leading three cubic oscillators ($n = 1,\ 2,\ 3$) in the neighborhood of the resonance of the linear oscillator $\Omega = 1$. The four plots from top to bottom in Fig. 2b show the average energies of the linear oscillator and the leading cubic oscillators, respectively. Note that in this case there is nonlinear targeted energy transfer from the linear oscillator to the hierarchical nonlinear chain of oscillators. Interestingly, a "chaotic band" is observed in the steady-state dynamics of the system since the responses of all nonlinear oscillators appear to be synchronized in the sense that they all become simultaneously "activated" (excited) to a chaotic state when the excitation frequency

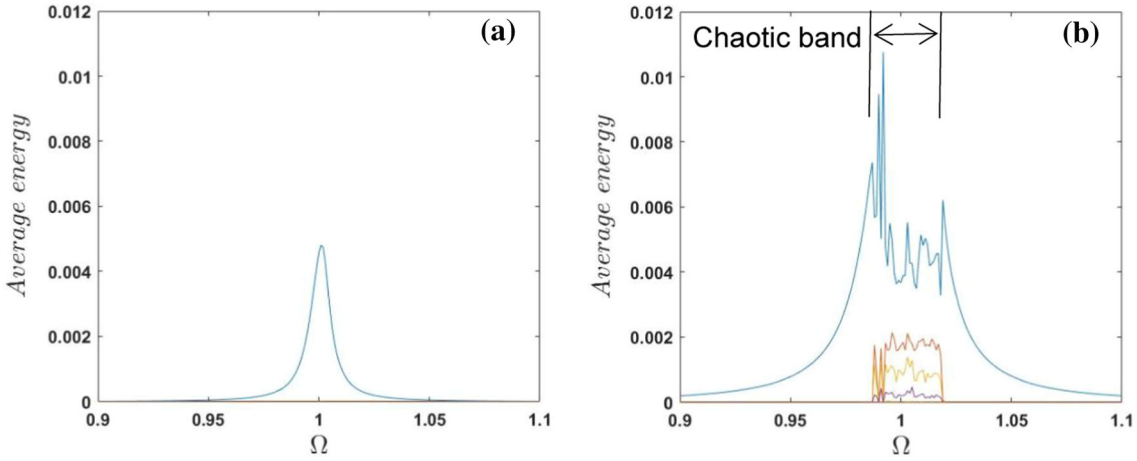

Fig. 2 Energy-frequency curves of the system of Fig. 1 for **a** weak excitation—$f = 0.001$, and **b** strong excitation—$f = 0.004$; the plots depict the average energies of the linear oscillator (top curve) and leading cubic oscillators (with their order increasing from top to bottom); note the "chaotic synchronization" inside the chaotic band in (**b**)

exceeds the lower critical threshold, $\Omega_l \approx 0.988$, and also simultaneously become "deactivated" above the upper critical threshold, $\Omega_u \approx 1.018$. Hence, a peculiar "chaotic synchronization" effect is observed in these results. We refer to the narrow frequency band where a sudden "burst" of the entire system to chaos occurs, as chaotic band. Clearly, the bounding frequencies of this chaotic band depend on energy, so they are expected to vary with the excitation amplitude; this was verified by numerical simulations for varying excitation amplitudes which are not shown here. In addition, examining the steady-state responses of the oscillators of the system within the chaotic band (cf. Fig. 3) it is concluded that the dynamics is irregular or chaotic; the chaotic nature of the steady-state dynamics in this response regime is proven by the Lyapunov exponent plots depicted in Fig. 4, verifying the existence of positive Lyapunov exponents in the responses.

Figure 3 depicts the time histories of the steady-state responses of the linear oscillator (LO) and the eight cubic oscillators (COs) for forcing amplitude $f = 0.004$ and frequency $\Omega = 1$ (in the chaotic band). Apart from the apparent irregular (chaotic) nature of these responses it is observed that the amplitudes of the COs are much larger than that of the LO, with the fourth CO exhibiting the largest response amplitude. Moreover, it is noted that the time histories of the responses of the leading four COs are significantly different, but those of the last four COs are similar so they appear to be synchronized in a certain sense. The reason for this effect is that the closer to the tail of the nonlinear chain, the smaller the mass of the CO. Consequently, the inertia forces of the last several COs are so small that they hardly produce any relative motions and are mainly "driven" by the chaotic dynamics of the leading COs.

In Fig. 4, the Lyapunov exponents of the nine oscillators of the system of Fig. 1 are depicted. The Lyapunov exponents are computed when the dynamics has reached the steady-state regime according to [23] where more details of the computation can be found. In this case, the normalized system (2) is cast into first-order equation form (i.e., in state-space form) involving eighteen variables, where nine variables are displacements and the other nine are the corresponding velocities. Accordingly, eighteen Lyapunov exponents are obtained, with each pair associated with the steady-state dynamics of each of the nine oscillators of the system. From Fig. 4 it is noted that thirteen Lyapunov exponents are positive, demonstrating that the system exhibits chaotic responses at steady state.

The chaotic nature of the steady-state response of the linear oscillator is further indicated by the irregular shape of the frequency response plot of the LO in Fig. 2b (which should be compared to the corresponding smooth plot of Fig. 2a), as well as the frequency response plots of the leading COs. Moreover, it is clear from the frequency response results that there is a finite (in frequency) chaotic frequency band where the entire system exhibits chaotic steady-state responses, and outside this band the steady-state responses are linearized and mainly confined to the directly forced LO; indeed, outside this band the responses of all COs are negligible, resembling the lower-amplitude excitation case of Fig. 2a. Therefore, the interesting phenomenon of "chaotic synchronization" of the nonlinear chain of cubic oscillators for a finite frequency band is observed in this system when the excitation amplitude exceeds a critical threshold.

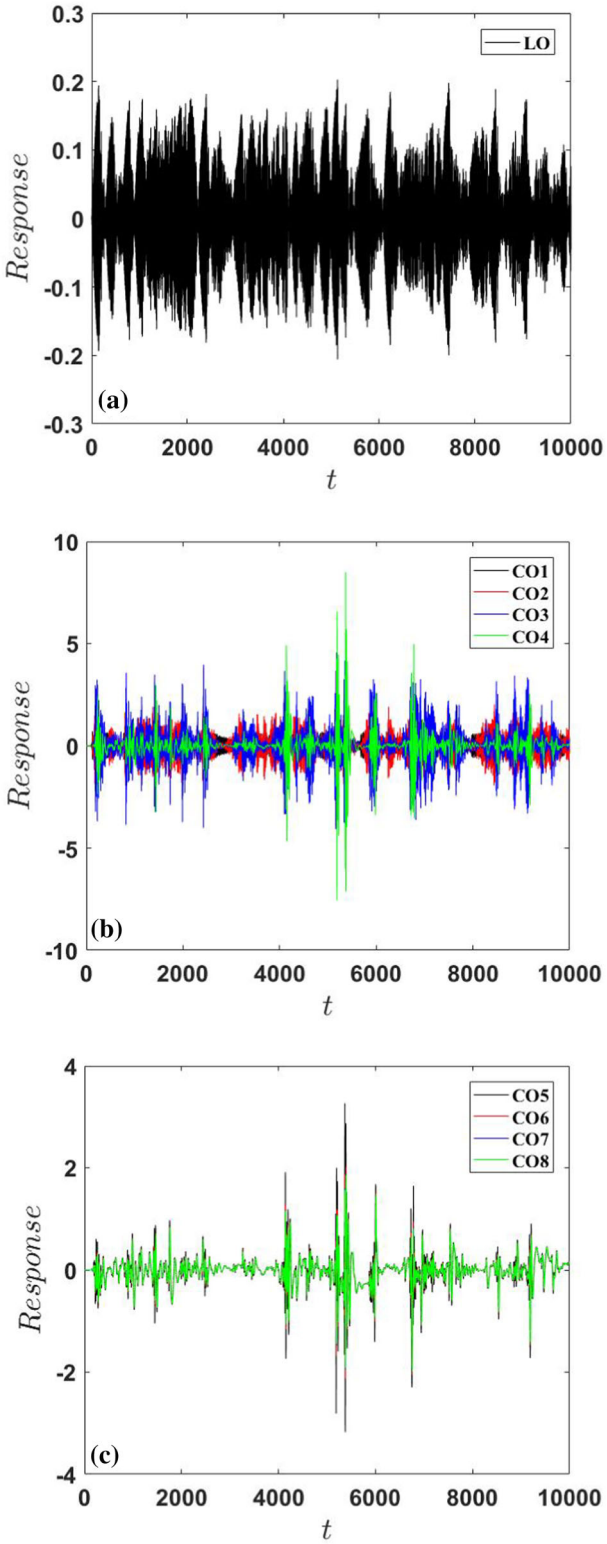

Fig. 3 Chaotic responses at steady state of the nine oscillators of the system inside the chaotic band for $f = 0.004$ and $\Omega = 1$: **a** Directly excited linear oscillator (LO), **b** cubic oscillators (COs) for $n = 1 - 4$, and **c** COs for $n = 5 - 8$

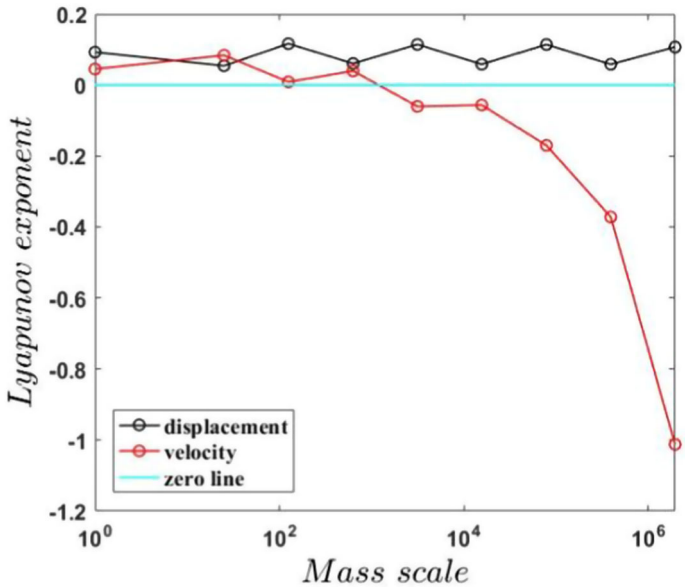

Fig. 4 Lyapunov exponents of nine oscillators inside the chaotic band for $f = 0.004$ and $\Omega = 1$, proving the chaotic nature of the time series of Fig. 3; the mass scales in this plot are defined as $1/\varepsilon_n$, $n = 1,\ 2\ \cdots\ N$, with the mass scale corresponding to the linear oscillator normalized to unity

In Fig. 5, the resulting irreversible energy cascade from the directly excited large-scale linear oscillator to the smaller-scale cubic oscillators of the attached chain is depicted at $\Omega = 1$ (inside the chaotic band) and two different excitation amplitudes. Depicted in this Figure are the average energy and normalized energy flux, which are based on Eqs. (3) and (4.2), respectively. These energy measures (averages) are depicted after the system has reached a steady state – this was ensured by considering the dynamics starting from an initial time $t_0 = 7,000$ and for a time window $T = 3,000$. In Fig. 5a the average energies of the mass scales (oscillators) are depicted, whereas in Fig. 5b the normalized energy fluxes between adjacent mass scales are examined—with the energy flux between the excited linear oscillator and its adjacent cubic oscillator normalized to unity. The cascade corresponding to the lower excitation level ($f = 0.001$) corresponds to periodic responses of the system, whereas the cascade realized at the higher excitation level ($f = 0.004$) to chaotic responses. The well-known Kolmogorov energy cascade (the so-called “–5/3 law”) for fully developed turbulence is also presented in Fig. 5a, to provide a qualitative comparison between the energy cascades realized in the present mechanical system with cubic nonlinearities, and the corresponding irreversible large-to-small scale energy transfers caused by the quadratic nonlinearities of the Navier–Stokes equations in turbulent flows. A first general conclusion from these results is that, irrespective of the level of excitation, a sustained large-to-small scale energy cascade is realized in the system of Fig. 1. This is caused by the strong cubic nonlinearity of the attached hierarchical chain of oscillators, and, as shown in [24] is caused by the nonlinear frequency-amplitude relationships of the cubic oscillators which dictates the realization of sustained resonance capture in each oscillator depending on its scale. It is interesting to note that the combination of strong nonlinearity and scale hierarchy (asymmetry) yields intense acoustic non-reciprocity in this system [24].

Examining in more detail the energy cascades of Fig. 5a it is observed that the realized large-to-small scale energy cascades are quite different for the cases of periodic and chaotic responses. Indeed, for low forcing amplitude the energy cascade is weak, as evidenced by its small logarithmic slope. For high forcing amplitude, however, the energy cascade is much more intense, and for the smaller scale cubic oscillators it resembles Kolmogorov’s law in slope. Specifically, following an initial nearly constant energy cascade from the linear oscillator to the leading cubic oscillators of the hierarchical chain, the energy cascade settles into a nearly linear logarithmic slope which is approximately equal to the –5/3 slope of Kolmogorov’s law. Considering the normalized energy fluxes depicted in Fig. 5b, quantifying the steady state energy transfer in the nonlinear chain, it is noted that the much more intense normalized energy flux occurs for stronger excitation, which is nearly constant between the leading cubic oscillators before settling to smaller values for the smaller scale oscillators of the hierarchical chain. Compared to the smaller energy fluxes in the regime of periodic responses (for the smaller forcing amplitude) it is concluded that the cross-scale energy transfers are significantly enhanced in the

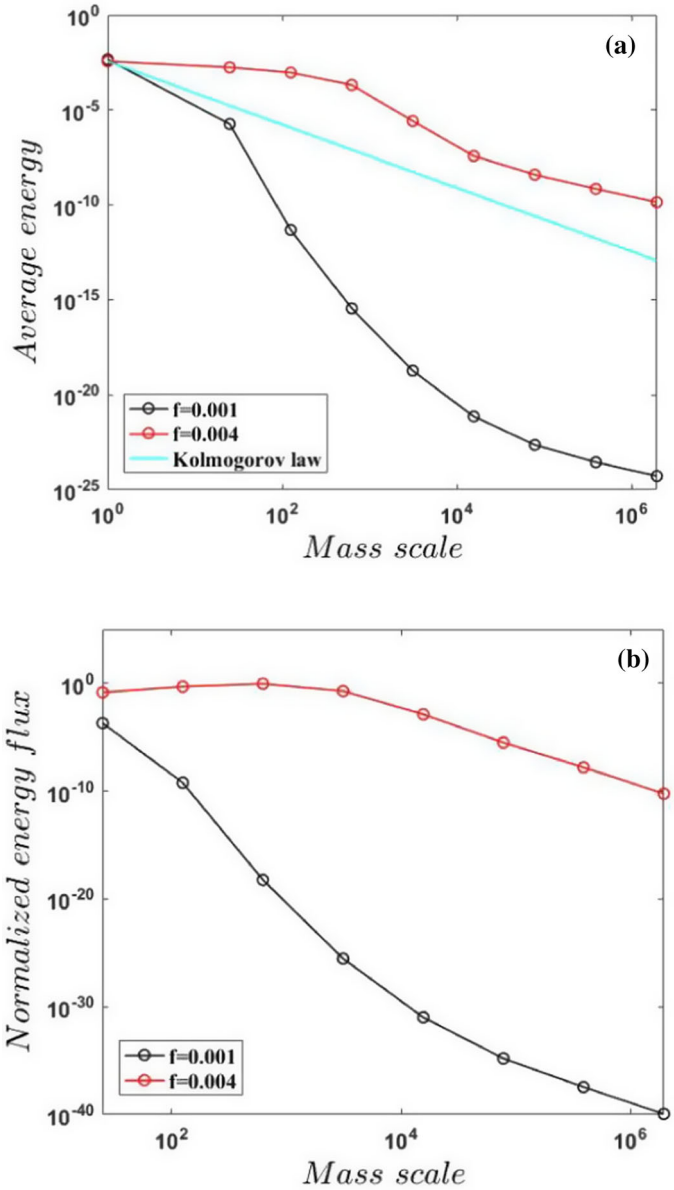

Fig. 5 Large-to-small scale nonlinear energy cascading and energy transfer at two excitation levels and $\Omega = 1$ (inside the chaotic band): **a** Average energies—see relations (3), and **b** normalized energy fluxes—see relations (4.2), versus mass scales (oscillators); for comparison the Kolmogorov –5/3 energy cascade for fully developed turbulence is depicted in (**a**)

regime of chaotic responses (for the larger forcing amplitude). Hence, for a sufficiently high excitation level, a rather intense steady state cross-scale energy transfer is realized across the nonlinear hierarchical chain.

To gain insight into the chaotic dynamics for the case of high excitation level ($f = 0.004$ and $\Omega = 1$), in Fig. 6 the coupling forces F_n (the sum of the stiffness and dissipative forces) versus the relative displacements and velocities, respectively, for the linear and cubic oscillators of the system are presented. In this way, the role of cubic stiffness nonlinearities and the linear viscous dissipative forces in the energy transfer process can be investigated. To this end, the stiffness forces, F_{sn}, and dissipative forces, F_{dn}, between the $n-th$ and $(n+1)-th$ oscillators are computed to be

$$F_n = F_{sn} + F_{dn} \equiv k_n(x_n - x_{n+1})^3 + \lambda_n(\dot{x}_n - \dot{x}_{n+1}), n = 1,\ 2 \ldots N. \tag{5}$$

The results show that the chaotic dynamics of the three leading (larger scale) cubic oscillators (cf. Fig. 6a-c) are mainly dominated by the strong stiffness nonlinearity, while the dynamics of the last four (smaller scale)

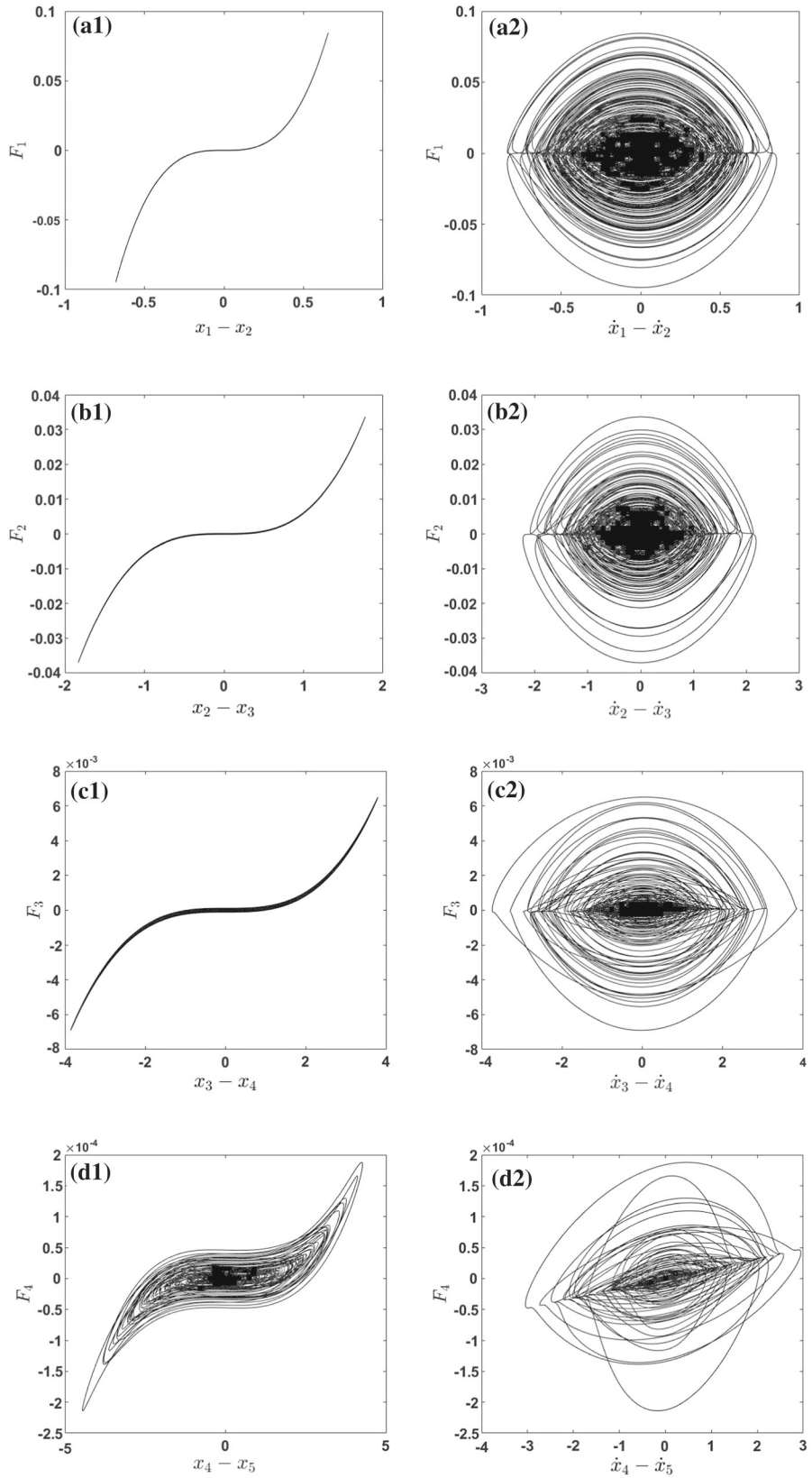

Fig. 6 Steady state coupling force F_n versus relative displacement $(x_n - x_{n+1})$, and relative velocity $(\dot{x}_n - \dot{x}_{n+1})$ in the chaotic regime of the hierarchical chain for $f = 0.004$ and $\Omega = 1$

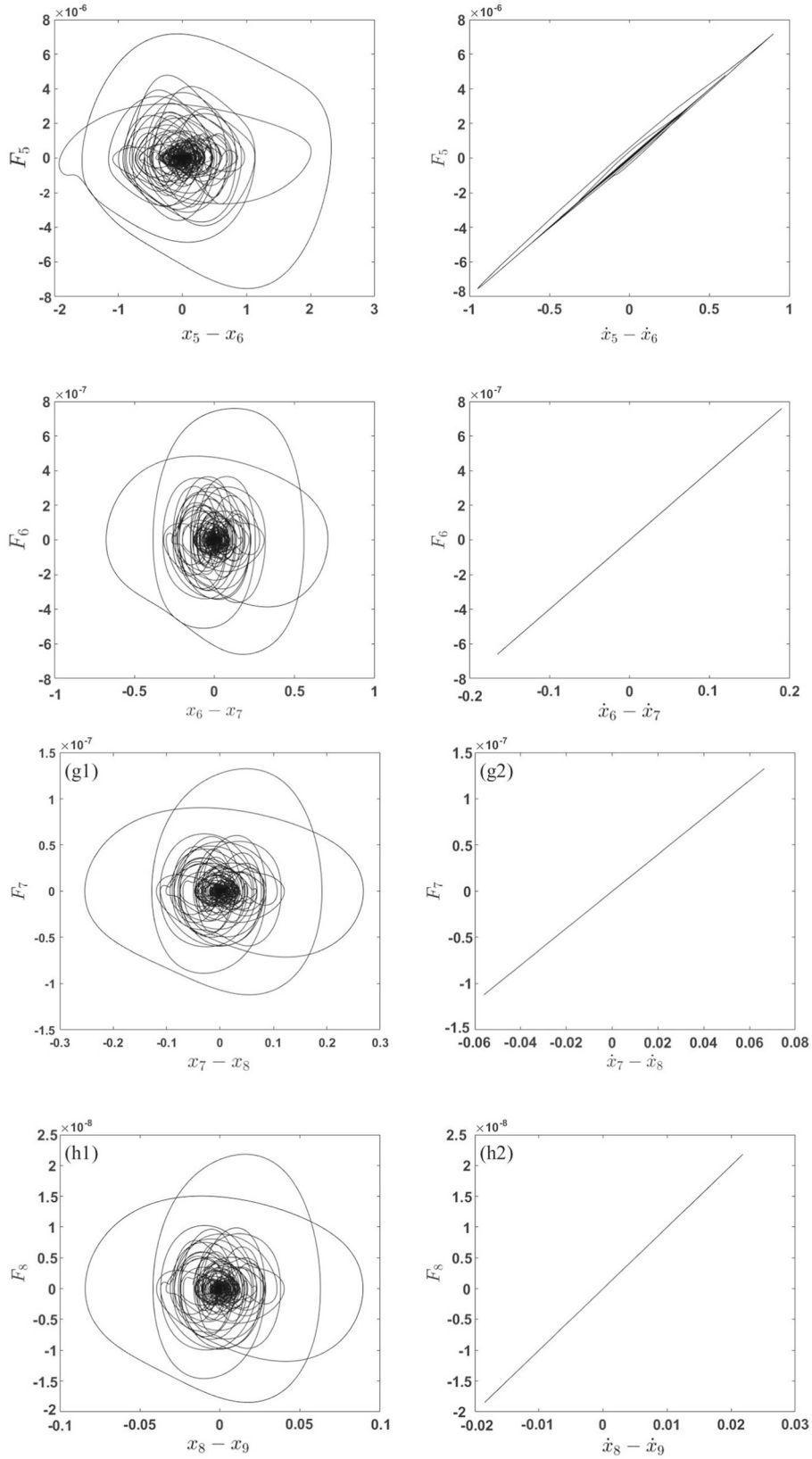

Fig. 6 continued

cubic oscillators (cf. Fig. 6e-h) are mainly influenced by the linear viscous dissipation. The dynamics of the fourth cubic oscillator (cf. Fig. 6d) represents a transition between these two different chaotic states. Hence, it appears that the last few smaller scale oscillators are mainly "driven" by the larger scale ones and their dynamics are primarily governed by viscous damping. These results correlate with the energy cascade for $f = 0.004$ depicted in Fig. 5a. In particular, this cascade can be divided into two main parts, that is, an initial nearly horizontal part for the leading larger scale oscillators, and a Kolmogorov-like power law part for the last smaller scale oscillators; the transition between these two parts corresponds to the coupling forces F_{s4} and F_{d4} depicted in Fig. 6d. Accordingly, it seems that the Kolmogorov-type cascade in Fig. 5a corresponds to the damping-dominated chaotic dynamics of the smaller scale cubic oscillators in the hierarchical chain. From the above discussion we can see several analogies with the energy transfers observed in fully developed turbulence. Specifically, the energy is injected to the large-scale spatial modes either due to the applied forcing or to instability (similarly with the three leading oscillators). Subsequently it is continuously transferred due to nonlinearity in smaller scales, where dissipation dominates. Between the (larger) scales where we have pure energy transfer due to the nonlinear effects (termed the inertial scales) and the (smaller) scales that are dissipation-dominated (termed the dissipation scales) there is a transition regime, similar to the mechanical system analyzed here.

To investigate the energy cascade and transfer in the chaotic steady-state regime, the excitation frequency was fixed to $\Omega = 1$, and the excitation magnitude f was varied in the range [0.003, 0.02]. The results are depicted in Fig. 7, and it is concluded that when the hierarchical nonlinear chain enters into the chaotic state, a characteristic correlation forms between energy and mass scale, consisting of an almost horizontal initial part followed by a latter part that obeys a near power law which resembles the Kolmogorov law (cf. Fig. 7a). Hence, the cascade depicted in Fig. 5a seems to be robust in the chaotic regime. Furthermore, the normalized nonlinear energy fluxes depicted in Fig. 7b indicate that the energy fluxes increase in the leading larger scale cubic oscillators, and then decrease for the smaller scale ones. We can again observe analogies with the case of fluid turbulence but also some differences. While in turbulence the flux of energy occurs, in general, from large to small scales, it has an almost constant rate. This is because in the inertia subrange the viscous dissipation effects are negligible, and energy is just transferred through it until it reaches the dissipation regime. On the other hand, for the case if the nonlinear mechanical chain energy flux is not a constant, at least over an equally lengthy mass range. Nevertheless, considering that the chaotic dynamics of the leading larger scale cubic oscillators are dominated by the stiffness nonlinearity, and that of the smaller scale oscillators by linear viscous damping (cf. Fig. 6), the results of Fig. 7b indicate that the activation of strongly nonlinear stiffness effects is the key factor for initiating the energy transfer (and cascading) process in the chaotic regime.

4 Case of two coupled linear oscillators

In this Section, we consider a variant of the hierarchical oscillator chain by considering two linear primary oscillators coupled to the same eight hierarchical cubic oscillators as described previously; the system is illustrated in Fig. 8. Given that under in-phase harmonic excitations of the two linear oscillators the dynamics of this augmented chain has similar dynamics and nonlinear energy cascades to those of the system with a single primary oscillator, here we focus exclusively on out-of-phase harmonic excitations; moreover, the system parameters are the same as those of the study in the previous Section.

The equations of motion for this system, take the non-dimensional form

$$\ddot{x}_1 + \tilde{\mu}\dot{x}_1 + x_1 + \tilde{\mu}(\dot{x}_1 - \dot{\overline{x}}_1) + (x_1 - \overline{x}_1) = \tilde{f}\cos(\tilde{\Omega}\tilde{t}), \tag{6.1}$$

$$\ddot{\overline{x}}_1 + \tilde{\mu}\left(\dot{\overline{x}}_1 - \dot{x}_1\right) + (\overline{x}_1 - x_1) + \lambda_1(\dot{\overline{x}}_1 - \dot{x}_2) + k_1(\overline{x}_1 - x_2)^3 = -\tilde{f}\cos(\tilde{\Omega}\tilde{t}), \tag{6.2}$$

$$\varepsilon_1\ddot{x}_2 + \lambda_1(\dot{x}_2 - \dot{\overline{x}}_1) + k_1(x_2 - \overline{x}_1)^3 + \lambda_2(\dot{x}_2 - \dot{x}_3) + k_2(x_2 - x_3)^3 = 0, \tag{6.3}$$

$$\varepsilon_n\ddot{x}_{n+1} + \tilde{\lambda}_n(\dot{x}_{n+1} - \dot{x}_n) + \tilde{k}_n(x_{n+1} - x_n)^3 + \tilde{\lambda}_{n+1}(\dot{x}_{n+1} - \dot{x}_{n+2}) + \tilde{k}_{n+1}(x_{n+1} - x_{n+2})^3 = 0,$$

$$n = 2\,,\ 3\ldots N-1, \tag{6.4}$$

$$\varepsilon_N\ddot{x}_{N+1} + \tilde{\lambda}_N(\dot{x}_{N+1} - \dot{x}_N) + \tilde{k}_N(x_{N+1} - x_N)^3 = 0, \tag{6.5}$$

where the previous normalizations hold, and the tildes are dropped in the following analysis for convenience. A relatively strong excitation level with $f = 0.02$ is considered to activate chaotic responses in the system.

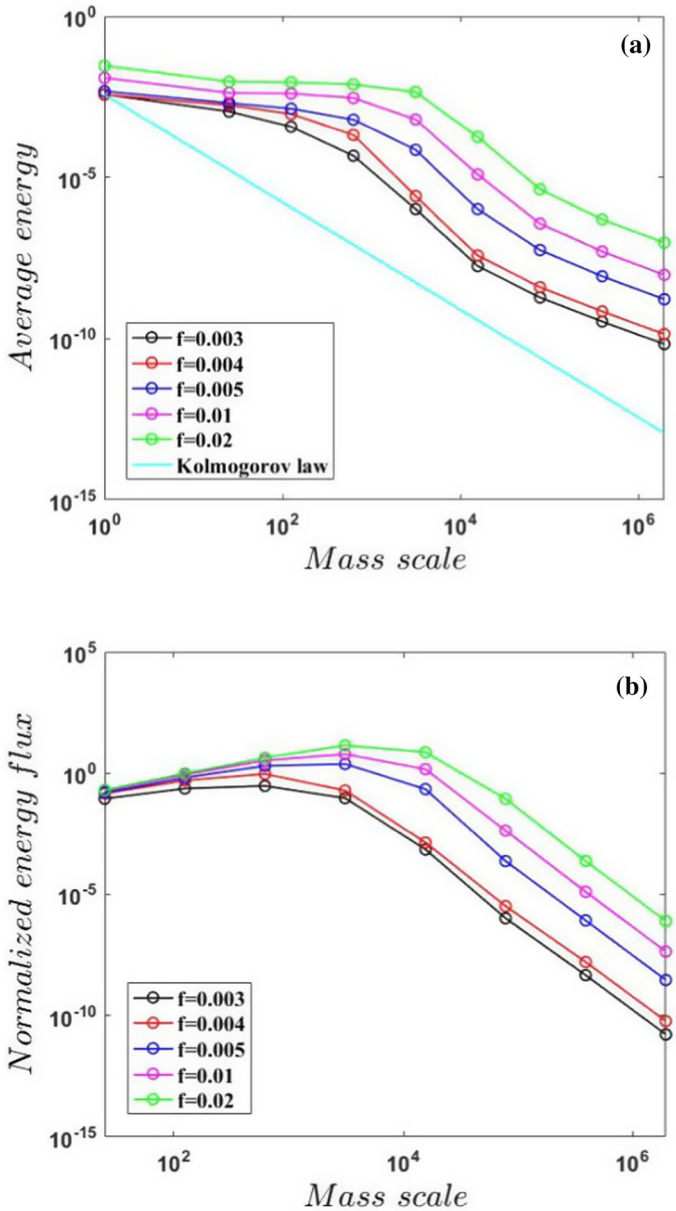

Fig. 7 Irreversible large-to-small scale nonlinear energy cascading and energy transfer for $\Omega = 1$ and varying force excitation level in the chaotic steady state regime: **a** average energies, and **b** normalized energy fluxes versus mass scales (oscillators); for comparison the Kolmogorov $-$ 5/3 energy cascade for fully developed turbulence is depicted in (**a**)

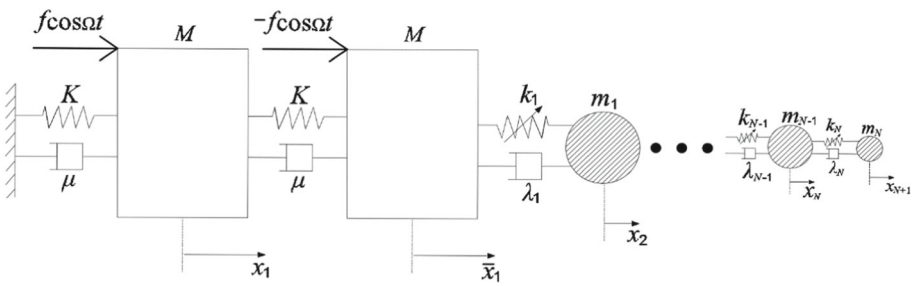

Fig. 8 Hierarchical chain with two linear primary oscillators subject to out-of-phase excitations

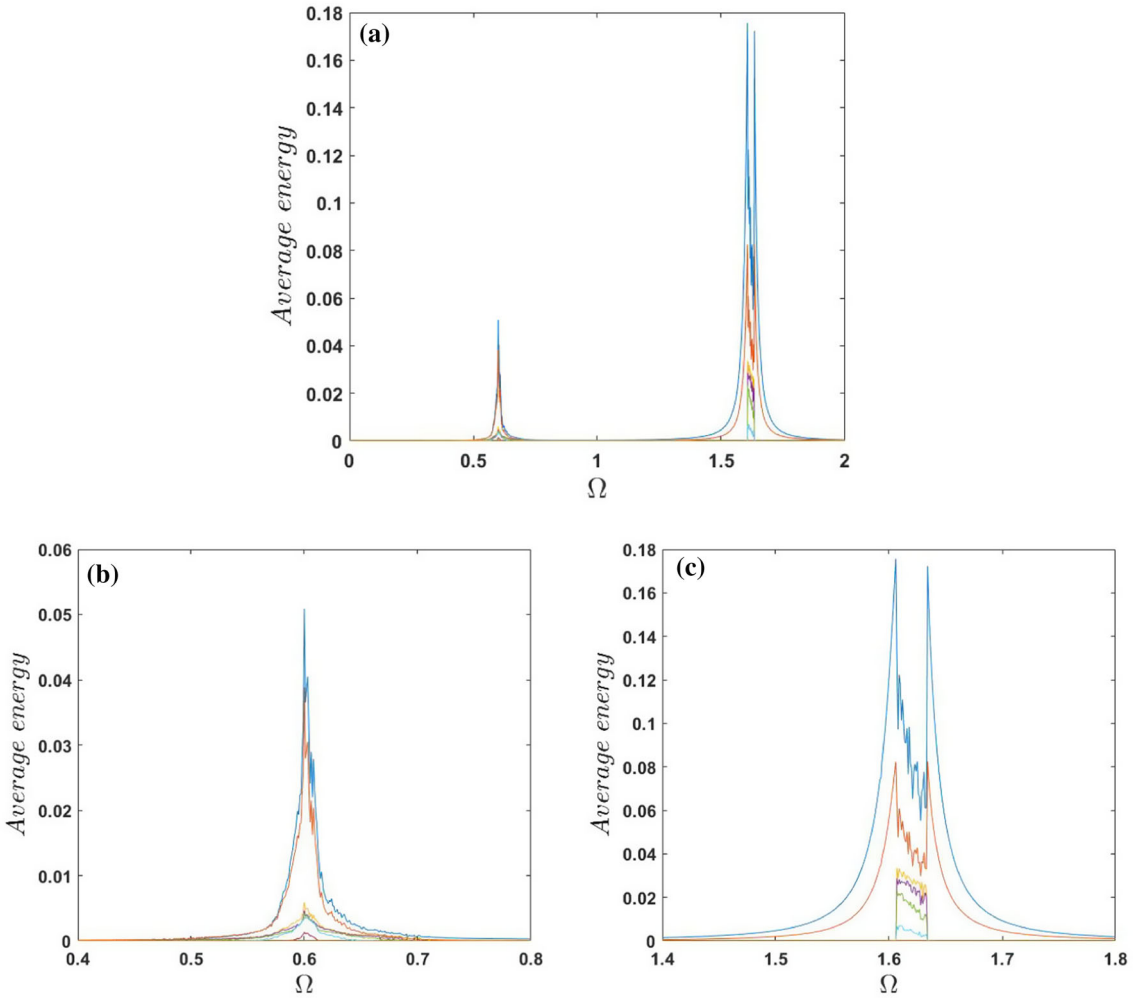

Fig. 9 Energy-frequency curves of the system of Fig. 8 for $f = 0.02$ and **a** $\Omega = 0 - 2$, **b** $\Omega = 0.4 - 0.8$ (detail in the lower resonance region), and **c** $\Omega = 1.4 - 1.8$ (detail in the higher resonance region); the plots depict the average energies of the linear oscillators (top curves) and leading cubic oscillators (with their orders increasing from top to bottom)

In Fig. 9, the frequency response plots of the ten oscillators are presented, and two enlarged Subfigures (cf. Fig. 9b and c) are given to highlight the chaotic frequency bands. Similar to Fig. 2 for the case of a single linear primary oscillator, two chaotic bands are realized close to the two linearized resonances of the system. The bounding frequencies of the higher-frequency chaotic band are easily observed, and the resulting chaotic dynamics realized in that band drastically enhance the targeted energy transfer from the two linear oscillators to the hierarchical cubic oscillator chain. On the other hand, no such clear boundaries exist for the lower-frequency chaotic band, although chaotic oscillations are realized in that frequency range as well. Relatively speaking, the targeted energy transfer from the linear oscillators to the cubic chain is weaker around the first resonance frequency compared to the neighborhood of the second resonance frequency.
The steady-state chaotic responses of the system for two values of the excitation frequency, namely, $\Omega = 0.62$ in the first chaotic band, and $\Omega = 1.62$ in the other chaotic band, are depicted in Figs. 10 and 11, respectively. The corresponding Lyapunov exponents are shown in Fig. 12 where we note that several of these exponents are positive; since the two linear primary oscillators have identical masses (normalized to unity), four exponents (two for displacements and two for velocities) corresponding to the unit mass scale are shown in each of the two Subfigures of Fig. 12.

In Fig. 13, we depict the nonlinear energy cascades and energy fluxes realized at two excitation frequencies in the lower and higher chaotic regions. The methods for computing the average energy and normalized energy flux are similar to those used in Fig. 5. However, it should be noted that the potential energy of the first

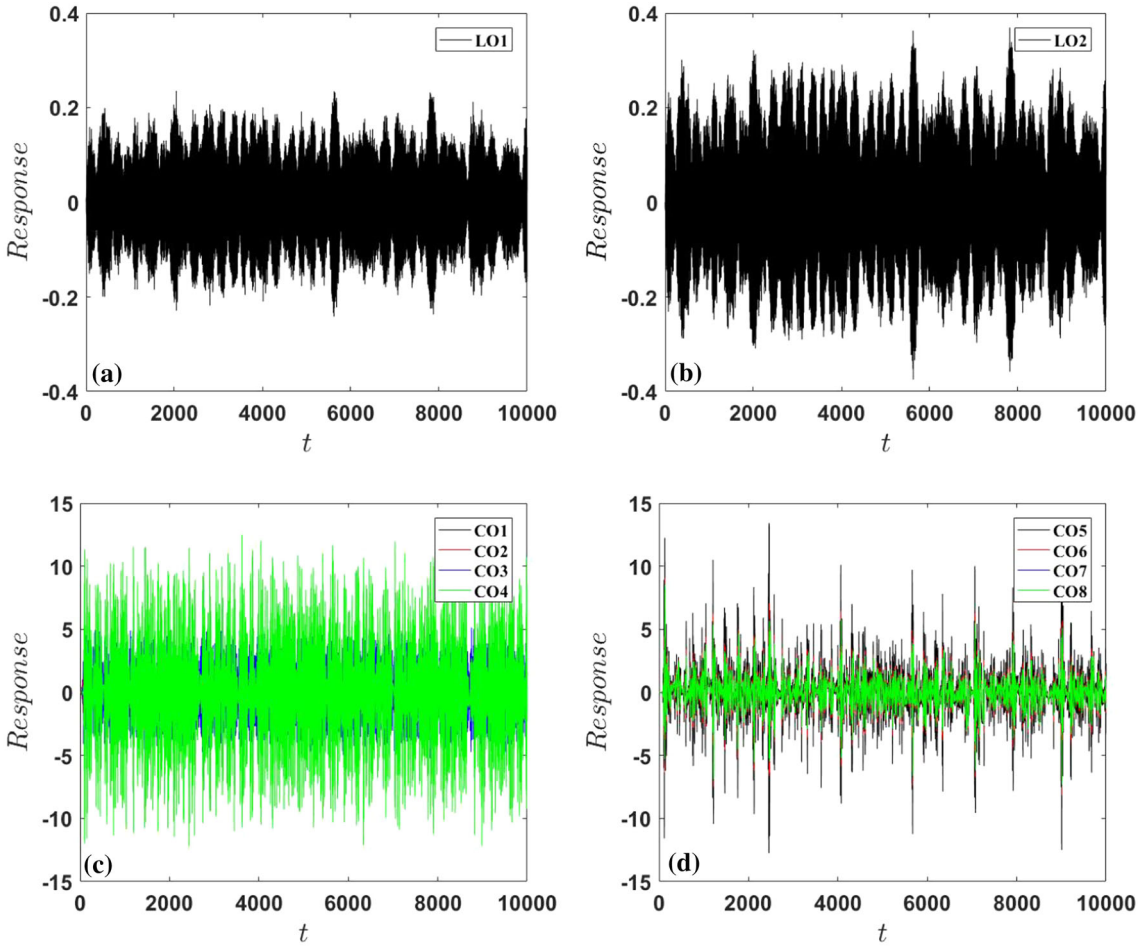

Fig. 10 Chaotic responses at steady state of the ten oscillators of the system for $f = 0.02$ and $\Omega = 0.62$ (lower-frequency chaotic regime): **a** the first linear oscillator (LO), **b** the second LO, **c** leading cubic oscillators (COs), $n = 1 - 4$, and **d** following COs, $n = 5 - 8$

linear oscillator is produced by its two adjacent linear stiffnesses. The results are analogous to the results observed in the system with a single primary linear oscillator (cf. Fig. 7), highlighting the robustness of these phenomena. Interestingly, although the average levels in the energy cascade at the lower-frequency chaotic region (for $\Omega = 0.62$) are lower compared to those in the higher-frequency one (for $\Omega = 1.62$)—cf. Fig. 13a, the corresponding energy fluxes in the lower-frequency region are higher—cf. Fig. 13b.

Finally, considering the coupling forces F_n as functions of the relative displacements and velocities, respectively, the observed trends are similar to the ones of Fig. 6 for the case of a single primary linear oscillator. In particular, the chaotic dynamics of the four leading cubic oscillators are mainly dominated by the strong stiffness nonlinearity, while the dynamics of the following four cubic oscillators are mainly influenced by the linear viscous dissipation. These results correlate fully with the energy cascades and fluxes depicted in Fig. 13. The nonlinear energy cascades in the two chaotic regions of Fig. 13a are divided into two parts, namely, an initial nearly horizontal part for the leading larger scale cubic oscillators—indicating near equipartition of energy between these oscillators are the chaotic steady state, followed by a later part obeying a Kolmogorov-like power law for the last smaller scale cubic oscillators. From the corresponding energy fluxes in Fig. 13b we note a monotonically increasing targeted energy transfer in the nonlinear stiffness dominated leading cubic oscillators, followed by a completely reversed monotonically decreasing sequence of energy fluxes as energy is directed and dissipated by the smaller-scale cubic oscillators. Hence, similar conclusions to the case of a SDOF primary linear oscillator can be drawn regarding the steady state nonlinear energy transfers in this system.

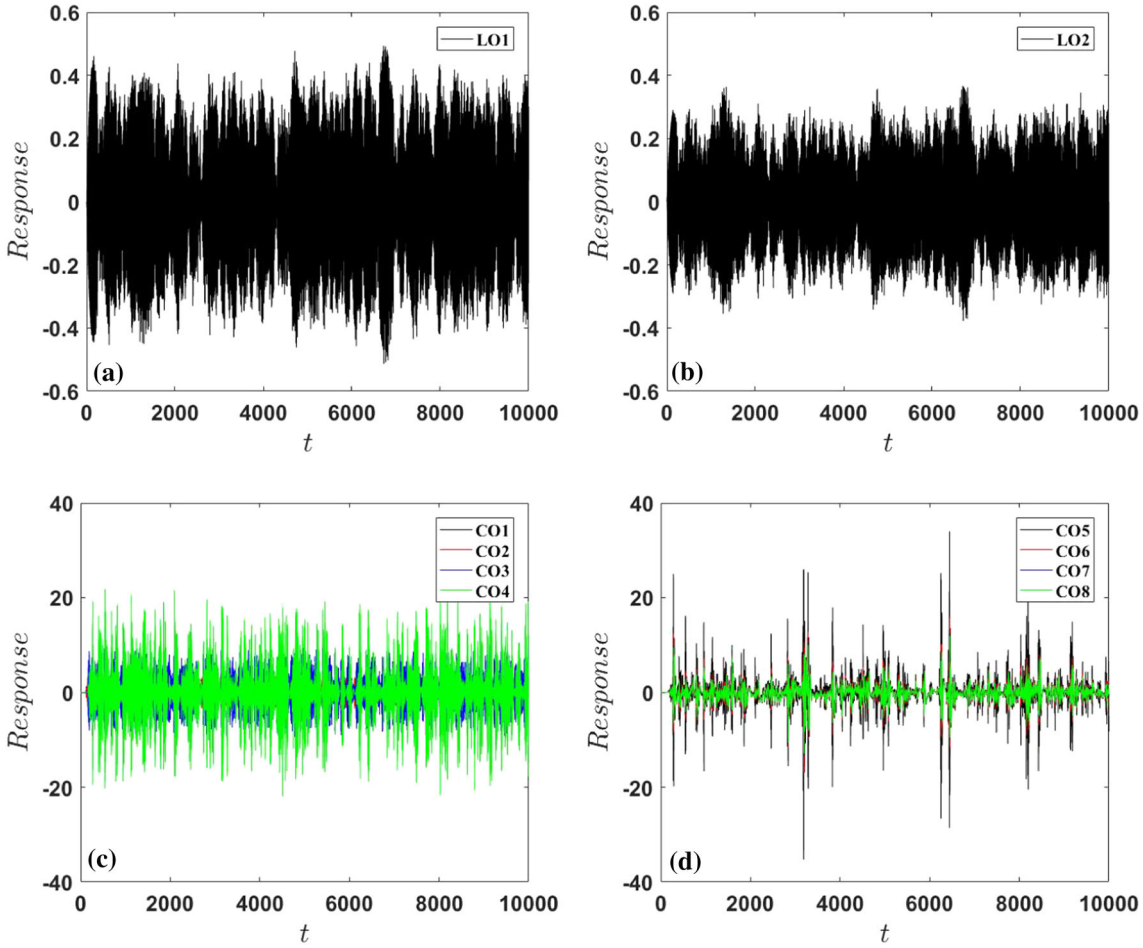

Fig. 11 Chaotic responses at steady state of the ten oscillators of the system for $f = 0.02$ and $\Omega = 1.62$ (higher-frequency chaotic band): **a** the first linear oscillator (LO), **b** the second LO, **c** leading cubic oscillators (COs), $n = 1 - 4$, and (d) following COs, $n = 5 - 8$

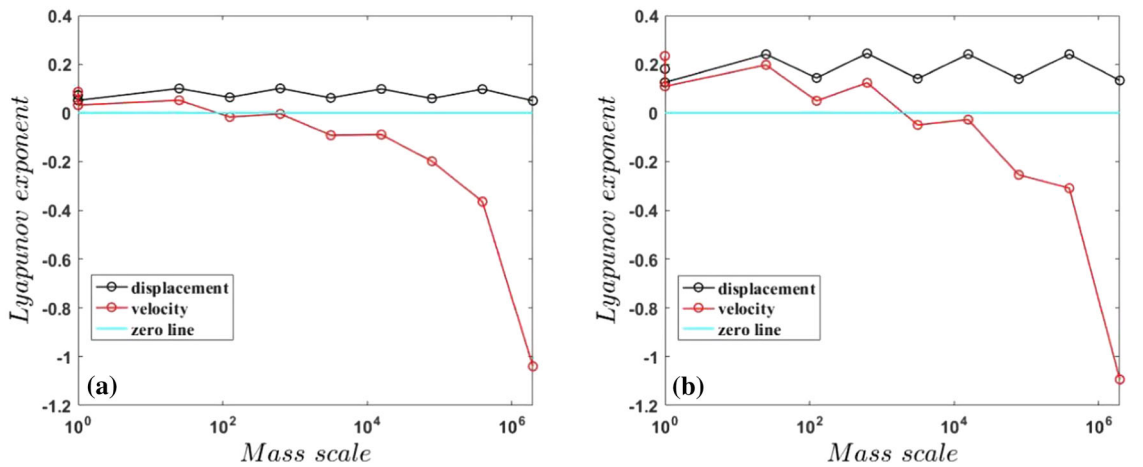

Fig. 12 Lyapunov exponents of the ten oscillators of the hierarchical nonlinear chain for $f = 0.02$ and **a** $\Omega = 0.62$ (lower-frequency chaotic regime), **b** $\Omega = 1.62$ (higher-frequency chaotic regime), proving the chaotic nature of the time series of Figs. 10 and 11

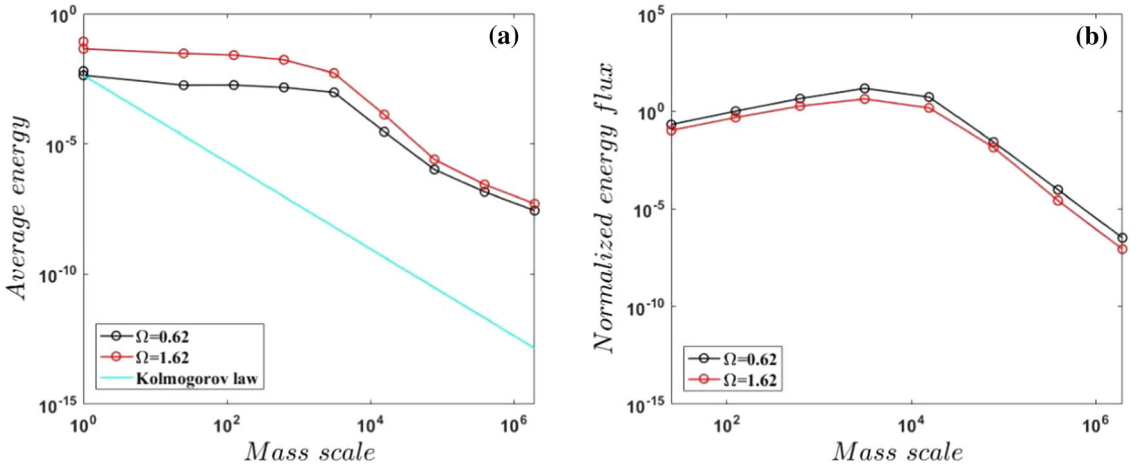

Fig. 13 Irreversible large-to-small scale nonlinear energy cascading and energy transfer at two excitation frequencies and $f = 0.02$: **a** Average energies—see relations (3), and **b** normalized energy fluxes—see relations (4.2), versus mass scales (oscillators)

5 Conclusions

We studied sustained energy cascades in the steady-state dynamical response of an hierarchical chain composed of one or two linear (primary) grounded oscillators coupled to a series of strongly, multi-scale ungrounded nonlinear oscillators with cubic stiffness characteristics and linear viscous dissipation, subject to harmonic force(s) applied to the linear oscillator(s).

At sufficiently low excitation levels, linear behavior prevails leading to nearly linear harmonic responses, where the mechanical energy remains localized in the directly forced linear oscillator. Exceeding a critical forcing threshold leads to chaotic responses of the chain and interesting sustained energy cascading from the large-scale cubic oscillators—whose dynamics is dominated by stiffness nonlinearity—to the small scale ones—whose dynamics is dominated by viscous dissipation. Moreover, these energy cascades are targeted, i.e., irreversible from large- to small-scales. It is noteworthy that there occurs a peculiar "chaotic synchronization," since all cubic oscillators are simultaneously entering or existing in the chaotic regime if a certain frequency band, i.e., as the excitation frequency varies.

When energy cascading is initiated in the chaotic regime, the smaller-scale cubic oscillators become driven by the chaotic dynamics of the larger-scale cubic oscillators. In addition, once the oscillator chain enters the chaotic response regime, the pattern of nonlinear energy cascading resembles (but is not identical to) the –5/3 Kolmogorov energy cascading power law observed in fully developed turbulence. There exist certain similarities and differences of the observed mechanical energy cascades and those realized in turbulent flows. Specifically, it is impressive how the nonlinearity plays a similar role in both cases, transferring energy through an instability mechanism and the associated chaotic dynamics. For both systems the higher scales (turbulence) and the higher masses (mechanical system) are dominated by energy-conserving nonlinearity, that is, nonlinear advection for fluids and nonlinear stiffness for the mechanical chain, while the smaller scales (turbulence) and smaller masses (mechanical system) are dominated by viscous dissipation or damping. However, in turbulence this flux has an almost constant rate, while for the nonlinear mechanical chain energy flux is not as constant, at least over an equally lengthy mass range.

The present study can be regarded as an attempt to study hierarchical lattice systems with features of "mechanical turbulence," i.e., with sustained targeted energy cascades, initiated by strong nonlinearity, yielding irreversible energy transfer from larger scales dominated by stiffness nonlinearity to smaller scales dominated by viscous dissipation. An interesting future application would be in the field of acoustic metamaterial with inherent properties for "mechanical turbulence," mimicking the strong dissipative behavior and robustness exhibited by fully developed turbulent flows.

Acknowledgements This work was supported in part by Grant No. 201908120069 from China Scholarship Council which supported the sabbatical leave of Jian'en Chen to the University of Illinois. This support is greatly acknowledged.

References

1. Richardson, L.F.: Weather prediction by numerical process. Cambridge University Press, Cambridge (1922)
2. Frisch, U.: Turbulence: The legacy of A.N. Kolmogorov. Cambridge University Press (1995)
3. Vakakis, A.F.: Passive nonlinear targeted energy transfer. Philos. Trans. R. Soc. A Math. Phys. Eng. Sci. **376**(2127), 20170132 (2018)
4. Ding, H., Chen, L.Q.: Designs, analysis, and applications of nonlinear energy sinks. Nonlinear Dyn. **100**(4), 3061–3107 (2020)
5. Lu, Z., Wang, Z.X., Zhou, Y., Lu, X.L.: Nonlinear dissipative devices in structural vibration control: a review. J. Sound Vib. **423**, 18–49 (2018)
6. Balaji, P.S., Karthik SelvaKumar, K.: Applications of nonlinearity in passive vibration control: a review. J. Vib. Eng. Technol. **9**, 183–213 (2020)
7. Quinn, D.D., Triplett, A.L., Bergman, L.A., Vakakis, A.F.: Comparing linear and essentially nonlinear vibration-based energy harvesting. J. Vib. Acoustics **133**(1), 011001 (2011)
8. Zang, J., Cao, R.Q., Zhang, Y.W., Fang, B., Chen, L.Q.: A lever-enhanced nonlinear energy sink absorber harvesting vibratory energy via giant magnetostrictive-piezoelectricity. Commun. Nonlinear Sci. Numer. Simul. **95**, 105620 (2021)
9. Mojahed, A., Gendelman, O.V., Vakakis, A.F.: Breather arrest, localization, and acoustic non-reciprocity in dissipative nonlinear lattices. J. Acoust. Soc. Am. **146**(1), 826–842 (2019)
10. Bunyan, J., Moore, K.J., Mojahed, A., Fronk, M.D., Leamy, M., Tawfick, S., Vakakis, A.F.: Acoustic nonreciprocity in a lattice incorporating nonlinearity, asymmetry, and internal scale hierarchy: experimental study. Phys. Rev. E **97**(5), 052211 (2018)
11. Ditlevsen, P.D.: Turbulence and shell models. Cambridge University Press, Cambridge (2010)
12. Munoz, V., Dominguez, M., Nigro, G., Riquelme, M., Carbone, V.: Fractality of an MHD shell model for turbulent plasma driven by solar wind data: a review. J. Atmos. Solar-Terr. Phys. **214**, 105524 (2021)
13. Bak, B.D., Kalmar-Nagy, T.: A linear model of turbulence: reproducing the Kolmogorov-spectrum. IFAC PapersOnLine **51**(2), 595–600 (2018)
14. Kalmar-Nagy, T., Bak, B.D.: An intriguing analogy of Kolmogorov’s scaling law in a hierarchical mass-spring-damper model. Nonlinear Dyn. **95**(4), 3193–3203 (2019)
15. Bak, B.D., Kalmar-Nagy, T.: Energy cascade in a nonlinear mechanistic model of turbulence. Tech. Mech. **39**(1), 64–71 (2019)
16. Düring, G., Krstulovic, G.: Exact result in strong wave turbulence of thin elastic plates. Phys. Rev. E **97**, 020201(R) (2018)
17. Humbert, T., Josserand, C., Touzé, C., Cadot, O.: Phenomenological model for predicting stationary and non-stationary spectra of wave turbulence in vibrating plates. Phys. D **316**, 34–42 (2016)
18. Humbert, T., Cadot, O., Düring, G., Josserand, C., Rica, S., Touzé, C.: Wave turbulence in vibrating plates: the effect of damping. Europhys. Lett. **102**, 30002 (2013)
19. Boudaoud, A., Cadot, O., Odille, B., Touzé, C.: Observation of wave turbulence in vibrating plates. Phys. Rev. Lett. **100**, 234504 (2008)
20. Mordant, N.: Are there waves in elastic wave turbulence? Phys. Rev. Lett. **100**(23), 234505 (2008)
21. Pikovsky, A., Rosenblum, M., Kurths, J.: Synchronization: a universal concept in nonlinear sciences. Cambridge University Press, Cambridge, UK (2001)
22. Pecora, L.M., Carroll, T.L.: Synchronization in chaotic systems. Phys. Rev. Lett. **64**(8), 821–824 (1990)
23. Argyris, J.H., Friedrich, R., Haase, M., Faust, G.: An exploration of dynamical systems and chaos: completely revised and enlarged, 2nd edn. Springer, Berlin (2015)
24. Moore, K.J., Bunyan, J., Tawfick, S., Gendelman, O.V., Li, S., Leamy, M., Vakakis, A.F.: Nonreciprocity in the dynamics of coupled oscillators with nonlinearity, asymmetry, and scale hierarchy. Phys. Rev. E **97**, 012219 (2018)